



Effect of β -Cyclodextrin on Physicochemical Properties of an Ionic Liquid Electrolyte Composed of *N*-Methyl-*N*-Propylpyrrolidinium bis(trifluoromethylsulfonyl)amide

Mio Suzuki, Naoya Kurahashi, Yuko Takeoka, Masahiro Rikukawa and Masahiro Yoshizawa-Fujita*

Department of Materials and Life Sciences, Sophia University, Tokyo, Japan

OPEN ACCESS

Edited by:

Jason B. Harper,
University of New South Wales,
Australia

Reviewed by:

Simonetta Antonaroli,
University of Rome Tor Vergata, Italy
Federica Valentini,
Università di Roma Tor Vergata, Italy

*Correspondence:

Masahiro Yoshizawa-Fujita
masahi-f@sophia.ac.jp

Specialty section:

This article was submitted to
Green and Sustainable Chemistry,
a section of the journal
Frontiers in Chemistry

Received: 27 September 2018

Accepted: 04 February 2019

Published: 20 February 2019

Citation:

Suzuki M, Kurahashi N, Takeoka Y, Rikukawa M and Yoshizawa-Fujita M (2019) Effect of β -Cyclodextrin on Physicochemical Properties of an Ionic Liquid Electrolyte Composed of *N*-Methyl-*N*-Propylpyrrolidinium bis(trifluoromethylsulfonyl)amide. *Front. Chem.* 7:90. doi: 10.3389/fchem.2019.00090

Ionic liquids (ILs) are promising electrolyte materials for developing next-generation rechargeable batteries. In order to improve their properties, several kinds of additives have been investigated. In this study, β -cyclodextrin (β -CD) was chosen as a new additive in IL electrolytes because it can form an inclusion complex with bis(trifluoromethylsulfonyl)amide (TFSA) anions. We prepared the composites by mixing *N*-methyl-*N*-propylpyrrolidinium bis(trifluoromethylsulfonyl)amide/LiTFSA and a given amount of triacetyl- β -cyclodextrin (Ac β -CD). The thermal behaviors and electrochemical properties of the composites were analyzed by several techniques. In addition, pulse field gradient NMR measurements were conducted to determine the self-diffusion coefficients of the component ions. The addition of Ac β -CD to the IL electrolytes results in the decrease in the conductivity value and the increase in the viscosity value. In contrast, the addition of Ac β -CD to the IL electrolytes induced an improvement in the anodic stability because of the formation of an inclusion complex between the Ac β -CD and TFSA anions. CDs are potential candidates as additives in IL electrolytes for electrochemical applications.

Keywords: ionic liquids, pyrrolidinium, TFSA, β -cyclodextrin, inclusion complex

INTRODUCTION

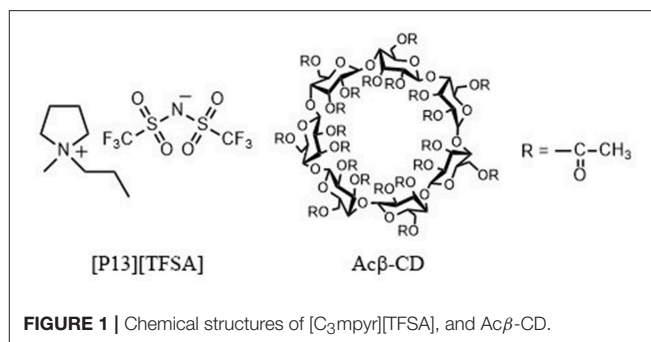
Ionic liquids (ILs) have been attractive as electrolyte materials because of their unique properties such as high ionic conductivity at room temperature and wide potential window (Armand et al., 2009). In addition, as ILs have a low vapor pressure and low flammability, they will be suitable for developing safer electrolytes instead of organic solvents (Ohno, 2011). Among onium cations, pyrrolidinium-based ILs are primarily being used as electrolytes in rechargeable batteries (Ishikawa et al., 2006; Matsumoto et al., 2006; Seki et al., 2008; Yoon et al., 2015). Pyrrolidinium-based ILs are superior in thermal and electrochemical stability as compared to those of other onium-based ILs. However, it is difficult to realize target ion transport with ions such as lithium ions or sodium ions in ILs, because the component ions of ILs as solvents also migrate along the potential gradient. New designs of ILs that address such drawback has been proposed by many researchers. For example, one candidate is poly(IL)s, which fix cation or anion species on the polymer chain (Yuan et al., 2013; Nishimura and Ohno, 2014; Qian et al., 2017). Another candidate is zwitterions, which have

the cation and anion in the same molecule (Yoshizawa et al., 2004; Narita et al., 2006; Yoshizawa-Fujita et al., 2011). Nevertheless, it is still difficult to achieve a high ionic conductivity over 10^{-2} S cm^{-1} at room temperature and a high lithium transference number (t_{Li^+}) over 0.5.

Rechargeable batteries, especially lithium-ion batteries (LIBs), employing ILs as the electrolyte materials have been developed (Ishikawa et al., 2006; Matsumoto et al., 2006; Seki et al., 2008; Ohno, 2011). For practical applications, a high energy density of LIBs is required. In order to improve the energy density of LIBs, the cells are needed to be operated at higher cut-off voltages. However, high cut-off voltages induce a significant decrease in the charge/discharge cycle stability of LIBs due to the decomposition of electrolytes. As a result, a passivation layer on the electrode is formed, even when ILs are used as electrolytes (Seki et al., 2008). The decomposition reaction of electrolytes should be suppressed at high cut-off voltages to allow the use of high-voltage cathode materials [e.g., $\text{LiCo}_{1/3}\text{Ni}_{1/3}\text{Mn}_{1/3}\text{O}_2$ (Yabuuchi and Ohzuku, 2003), $\text{LiNi}_{0.5}\text{Mn}_{1.5}\text{O}_4$ (Zhu et al., 2014)]. Various additives have been used to improve the anodic stability of electrolyte materials (Franco, 2015).

Cyclodextrin (CD) is a circular oligosaccharide composed of α -D(+)-glucopyranose units. The CD, which possesses seven glucose units, is called β -CD. They have a three-dimensional funnel-shaped architecture with a narrower rim molded by a hydrogen-bonding network built by primary OH groups (one group per glucose unit), and with a broader rim composed of secondary OH groups (two groups per glucose unit) (Crini, 2014). The two rims of the molecules are hydrophilic, while the interior of their cavity is hydrophobic. It is known that β -CD tends to form inclusion complexes with guest molecules with suitable characteristics of polarity and dimension in aqueous solutions (Silva et al., 2008; Baâzaoui et al., 2016). CD is among the most frequently used host molecule in supramolecular chemistry; this ability has been widely used in food and pharmaceutical studies (Szejtli, 1998; Crini, 2014). It has also been widely used in lithium battery research as a surfactant to effectively disperse solid substances in liquids and as an agent to promote complexation reactions, which is beneficial to material dispersion and molding (Chen et al., 2016).

Recently, Amajjahe et al. (2008) found that the anion of 1-butyl-3-vinylimidazolium bis(trifluoromethylsulfonyl)amide exclusively formed a host-guest complex with β -CD (Amajjahe and Ritter, 2008; Amajjahe et al., 2008). He et al. (2009) investigated the interaction of hydrophobic ILs and β -CD in detail (He et al., 2009). They found that the imidazolium cation did not interact with β -CD while its long alkyl side chain did. In addition, hydrophobic anions with fluorine atoms could interact with β -CD, and the interaction between the bis(trifluoromethylsulfonyl)amide (TFSA) anion and β -CD was stronger than those of BF_4 and PF_6 anions. These results prompted us to investigate the effect of β -CD on the physicochemical properties of ILs, and we expected that the anion trap ability of β -CD would contribute to the enhancement of the Li-ion conductivity and the improvement of the



electrochemical stability. In this study, a pyrrolidinium-based IL with a TFSA anion, *N*-methyl-*N*-propylpyrrolidinium bis(trifluoromethylsulfonyl)amide ([C₃mpyr][TFSA]) (see **Figure 1**), was used as the electrolyte solution. Its LiTFSA composites were prepared and mixed with different amounts of β -CD, and their physicochemical and electrochemical properties were evaluated.

EXPERIMENTAL

Materials

N-Methylpyrrolidine (Tokyo Chemical Industry Co., Ltd., > 98.0%), 1-chloropropane (Tokyo Chemical Industry Co., Ltd., > 99.0%), and lithium bis(trifluoromethylsulfonyl)amide (LiTFSA) (Kishida Chemical Co., Ltd., 99.0%) were purchased. *N*-Methylpyrrolidine and 1-chloropropane were purified by distillation *in vacuo* prior to use. Triacetyl- β -cyclodextrin (Ac β -CD) (Tokyo Chemical Industry Co., Ltd., > 97.0%) (see **Figure 1**) was used after drying.

[C₃mpyr][TFSA] was prepared as follows. *N*-Methyl-*N*-propylpyrrolidinium chloride ([C₃mpyr][Cl]) was synthesized according to a previously published procedure (Laus et al., 2008). [C₃mpyr][Cl] and LiTFSA were separately dissolved in deionized water. LiTFSA aq. was added dropwise to [C₃mpyr][Cl] aq. The resulting liquid was purified by washing repeatedly with deionized water until no residual chloride was detected with the use of AgNO_3 aq. [C₃mpyr][TFSA] was obtained as a colorless liquid at room temperature and characterized by ¹H NMR, fast atom bombardment mass spectrometry (FAB-MS), and elemental analysis. ¹H NMR (CD_2Cl_2 , 300 MHz): δ (ppm) = 3.50 (2H, ddd, $J = 10.22, 5.58, 3.01$ Hz), 3.26 (1H, dt, $J = 8.59, 4.04$ Hz), 3.04 (1.5H, s), 2.27 (2H, s), 1.83 (1H, tt, $J = 12.20, 5.61$ Hz), 1.06 (1.5H, t, $J = 7.39$ Hz). MS (FAB⁺): m/z 128.2 [M], 536.4 [2M+X]⁺, MS (FAB⁻): m/z 280.0 [X], 688.0 [M+2X]⁻. Anal. Calcd. for $\text{C}_{10}\text{H}_{18}\text{F}_6\text{N}_2\text{O}_4\text{S}_2$ (%): C, 29.4; H, 4.44; N, 6.86; S, 15.7; Found (%): C, 29.2; H, 4.42; N, 6.78; S, 16.1.

A given amount of LiTFSA was dissolved in [C₃mpyr][TFSA] [IL:LiTFSA = 18 : 1 (molar ratio)], and then a given amount of Ac β -CD was added into IL/LiTFSA composites at molar ratios LiTFSA:Ac β -CD = 1.0 : 0.5, 1.0 : 1.0, and 1.0 : 1.5. Four kinds of samples were prepared to investigate the effect of Ac β -CD on the properties of the IL electrolyte. Their composites are abbreviated

as the molar ratio of Ac β -CD. For example, the abbreviation of [C₃mpyr][TFSA]:LiTFSA:Ac β -CD = 18:1:1.5 is Ac β -CD1.5. These mixtures were stirred at 60°C for 24 h.

Measurements

Fourier-transform infrared (FT-IR) measurements were performed on a Nicolet 6700 (Thermo Fisher Scientific) by using KRS-5.

¹H and ¹⁹F NMR measurements were carried out with a Bruker Avance III HD 400 MHz at 25°C. Thermogravimetric analysis was conducted using a TG-DTA instrument (TG/DTA7200, Hitachi High-Technologies Corp.) under a nitrogen atmosphere at temperatures ranging from 25 to 500°C at a heating rate of 10°C min⁻¹. The thermal behavior was examined using differential scanning calorimetry (DSC) (DSC7020, Hitachi High-Technologies Corp.) at temperatures between -150 and 100°C at a heating/cooling rate of 10°C min⁻¹.

Impedance measurements were carried out using a VSP-300 (Bio-Logic Science Instruments) at frequencies ranging from 100 mHz to 1 MHz and temperatures ranging from 80 to -40°C. The temperature was controlled by a constant-temperature oven (SU-642, Espec Corp.). The composites were enclosed in a homemade glass cell having two platinum electrodes. The measurements were carried out by maintaining the cells at each temperature for 30 min. Viscosity measurements were carried out using a stabinger viscometer (SVM3000, Anton Paar) and temperature ranging from 80 to 20°C.

Pulse field gradient nuclear magnetic resonance (PFG-NMR) measurements were carried out with a Bruker Avance III HD 400 MHz at 80°C for ¹H, ⁷Li, and ¹⁹F nucleus. The ILs were filled into 5-mm NMR tubes, which were sealed. The measurements were carried out in 16 gradient steps per diffusion experiment. The gradient strength was 1,700 G cm⁻¹. The diffusion coefficients were calculated from the peak integration attenuation according to Equation 1 (Tanner and Stejskal, 1968):

$$A = A_0 - \exp[(\gamma\delta G)^2 D(\Delta - \frac{\delta}{3})] \quad (1)$$

where A is the signal at a certain gradient (G), A_0 is the signal at a gradient of 0, δ is the width of the gradient pulse, Δ is the diffusion time, D is the diffusion coefficient, and γ is the gyromagnetic ratio of the nuclei.

Linear sweep voltammetry (LSV) measurements were carried out by using a VSP-300 (Bio-Logic Science Instruments) in the potential range of -0.2 and 6 V at 60°C at a scan rate of 1.0 mV s⁻¹. Li foils were used as the reference and counter electrodes, while Ni and Pt plates were used as working electrodes in the potential ranges of -0.2–3.0, and 3.0–6.0 V, respectively. The electrodes were separated by a glass filter to prevent short-circuiting. The cyclic voltammetric measurements of [C₃mpyr][TFSA]:LiTFSA:Ac β -CD = 18:1:1.0 composites were carried out using a VSP-300 (Bio-Logic Science Instruments) in the potential range of -0.25–1.0 V at 25, at a scan rate of 1.0 mV s⁻¹, with Li foils as the reference and counter electrodes, and the Ni plate was used as the working electrode. The electrodes were separated by a glass filter to prevent short-circuiting.

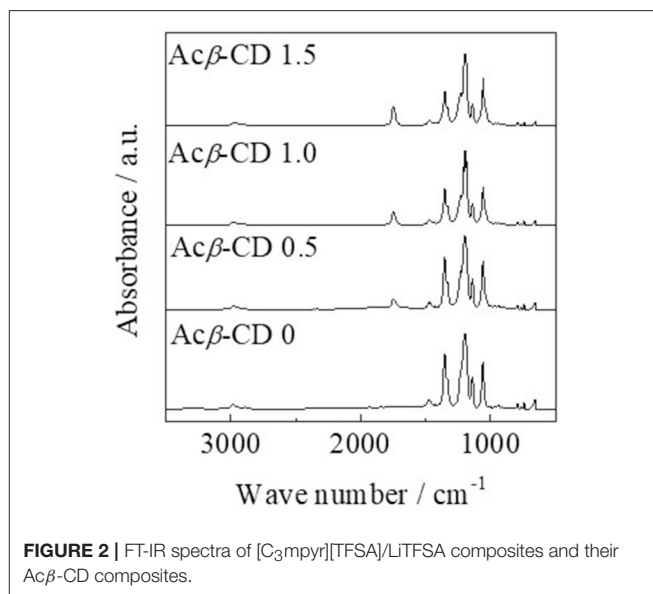


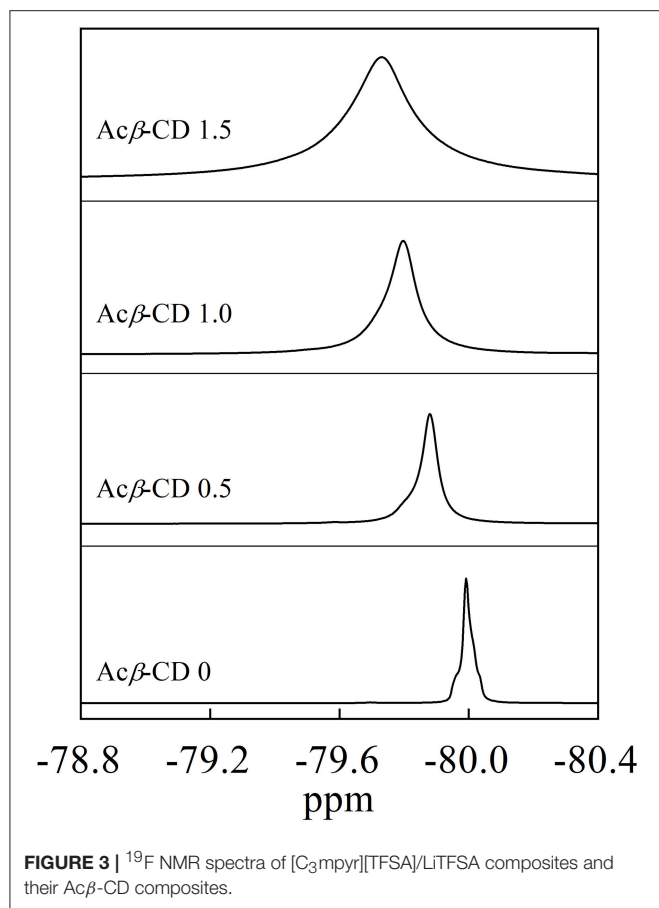
FIGURE 2 | FT-IR spectra of [C₃mpyr][TFSA]/LiTFSA composites and their Ac β -CD composites.

RESULTS AND DISCUSSION

Interaction Between Ac β -CD and TFSA Anion

A given amount of β -CD was initially added into [C₃mpyr][TFSA] and its LiTFSA mixture. Unfortunately, the IL electrolytes could not dissolve β -CD at any concentration. β -CD possesses hydroxyl groups, which form hydrogen bonds. The Lewis basicity of the TFSA anion is weak, and the TFSA anion cannot break the hydrogen bond. In fact, ILs with anions such as chloride and acetate, which exhibit a stronger Lewis basicity, can dissolve cellulose (Ohno and Fukaya, 2009) as such anions interact with the hydroxyl groups of cellulose because of the strong electron-donating ability. The TFSA anion could not dissolve even oligosaccharides. Therefore, Ac β -CD was used in this study instead of β -CD. A given amount of Ac β -CD was added into the IL electrolytes. [C₃mpyr][TFSA] with a weak Lewis-base anion could dissolve Ac β -CD, which has an acetyl group instead of a hydroxyl group.

FT-IR measurements were conducted, and each peak was assigned according to the literatures (Liu et al., 2009; Roy et al., 2016; Li et al., 2017; Wu et al., 2017). **Figure 2** presents FT-IR spectra of [C₃mpyr][TFSA]/LiTFSA and [C₃mpyr][TFSA]/LiTFSA/Ac β -CD composites. The FT-IR spectrum of [C₃mpyr][TFSA]/LiTFSA exhibits characteristic peaks for C-H stretching, CH₂ bending, and S=O stretching bands etc. The peaks in the range from 2,978 to 2,882 cm⁻¹ can be assigned to the C-H stretching and CH₂ bending modes. In the case of TFSA anion, the peaks of S=O stretching band and C-SO₂-N bond are observed at 1,349 and 1,136 cm⁻¹, respectively. In addition, CF₃ symmetric stretching modes are located in 1,195 cm⁻¹ and 1,056 cm⁻¹. For the spectrum of [C₃mpyr][TFSA]/LiTFSA/Ac β -CD, a new peak is observed at 1,746 cm⁻¹, which is assigned to C=O stretching mode for acetyl group, and the absorbance increases with increasing the Ac β -CD

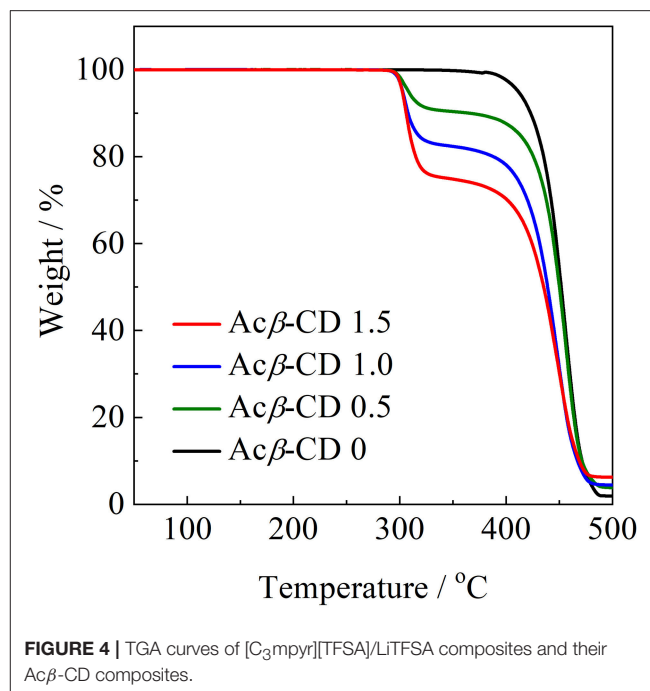


amount, indicating that the composites are formed by mixing $[\text{C}_3\text{mpyr}][\text{TFSA}]/\text{LiTFSA}$ and $\text{Ac}\beta\text{-CD}$.

^{19}F NMR measurements were carried out to investigate the interaction between $\text{Ac}\beta\text{-CD}$ and the TFSA anion. **Figure 3** presents ^{19}F NMR spectra of the CF_3 group in the TFSA anion for the $[\text{C}_3\text{mpyr}][\text{TFSA}]/\text{LiTFSA}$ and $[\text{C}_3\text{mpyr}][\text{TFSA}]/\text{LiTFSA}/\text{Ac}\beta\text{-CD}$ composites. The chemical shifts of the CF_3 group of the TFSA anion are -79.73 , -79.80 , -79.88 , and -79.99 ppm for the $\text{Ac}\beta\text{-CD}$ 1.5, 1.0, 0.5, and 0 composites, respectively. Zhang et al. (2014) performed ^{19}F NMR measurements of 1-ethyl-3-methylimidazolium bis(trifluoromethylsulfonyl)amide to detect the host-guest interaction between the $\beta\text{-CD}$ and TFSA anion (Zhang et al., 2014). As the molar ratio of CD increases, downfield shifts for the fluorine atom of the CF_3 group in the TFSA anion are observed because of the formation of the complex for CD and the TFSA anion. In all the $[\text{C}_3\text{mpyr}][\text{TFSA}]/\text{LiTFSA}/\text{Ac}\beta\text{-CD}$ composites, the CF_3 group chemically shifts to a lower magnetic field as compared to that of $\text{Ac}\beta\text{-CD}$ 0, suggesting that $\text{Ac}\beta\text{-CD}$ forms a complex with the TFSA anion.

Thermal Properties

To evaluate the thermal stability, onset thermal decomposition temperatures (T_d) were measured. **Figure 4** shows TGA traces for the $[\text{C}_3\text{mpyr}][\text{TFSA}]/\text{LiTFSA}$ and

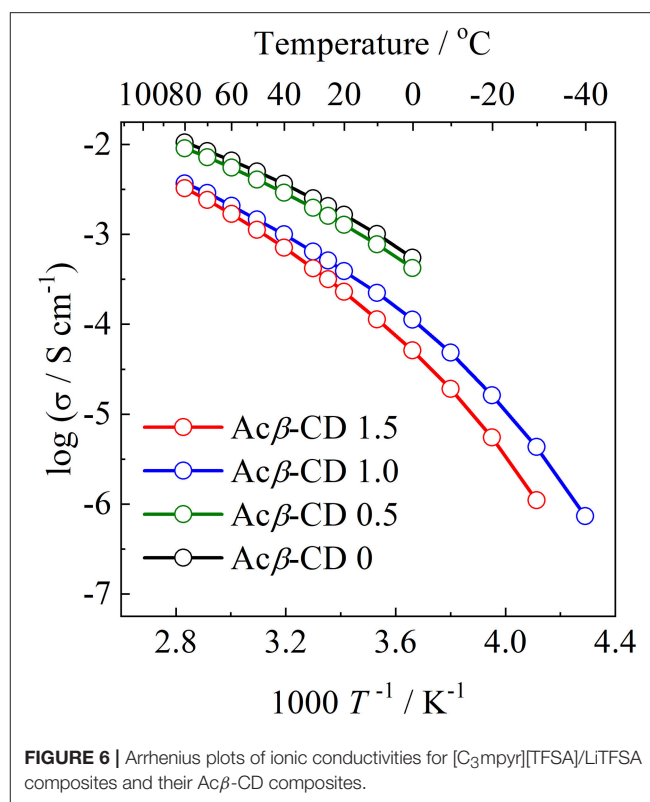
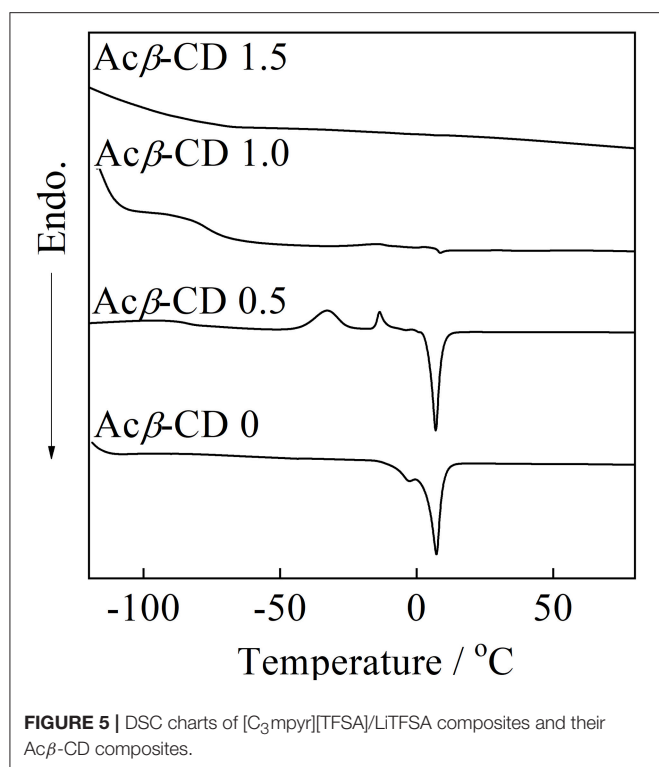


$[\text{C}_3\text{mpyr}][\text{TFSA}]/\text{LiTFSA}/\text{Ac}\beta\text{-CD}$ composites. $\text{Ac}\beta\text{-CD}$ 0 shows a T_d value at 386°C . Pyrrolidinium-based ILs with the TFSA anion are known to exhibit a higher thermal stability, and the T_d value of $\text{Ac}\beta\text{-CD}$ 0 is consistent with the literature value (Yang et al., 2014). All the composites with $\text{Ac}\beta\text{-CD}$ show similar T_d values, and their T_d values are about 300°C . This is due to the decomposition of $\text{Ac}\beta\text{-CD}$. The amount of weight loss is consistent with the amount of added $\text{Ac}\beta\text{-CD}$ in the IL electrolytes.

DSC traces of the composites are presented in **Figure 5**. $\text{Ac}\beta\text{-CD}$ 0 exhibits a melting point (T_m) of 8.0°C , which is consistent with the literature value (Wu et al., 2011). When the addition amount of $\text{Ac}\beta\text{-CD}$ is 0.5 in the molar ratio, the glass transition temperature (T_g), two crystallization temperatures, and T_m are observed at -91 , -33 , -19 , and 7.1°C , respectively. $\text{Ac}\beta\text{-CD}$ 0.5 exhibits no crystallization temperature upon the cooling scan. In addition, the T_m value of $\text{Ac}\beta\text{-CD}$ 0.5 slightly decreases as compared to that of $\text{Ac}\beta\text{-CD}$ 0. The crystallization temperature and T_m cannot be observed in the composites in which the added amount of $\text{Ac}\beta\text{-CD}$ is larger than the amount of Li salt in the molar ratio. $\text{Ac}\beta\text{-CD}$ 1.0 and 1.5 exhibits T_g only and maintains low values below -79°C . These results suggest that the interaction between the $\text{Ac}\beta\text{-CD}$ and TFSA anion prevents the crystallization of the IL.

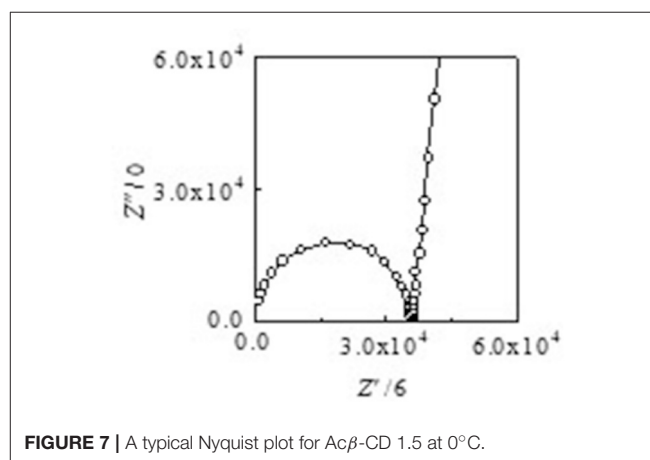
Conductivity and Viscosity

Arrhenius plots of the ionic conductivities for the composite electrolytes are presented in **Figure 6**. **Figure 7** exhibits a typical Nyquist plot for $\text{Ac}\beta\text{-CD}$ 1.5 at 0°C . The ionic conductivity values were calculated from the touchdown point on the Z' -axis which exhibits the resistance of the compound. For $\text{Ac}\beta\text{-CD}$ 0 and 0.5, the conductivity values were not obtained by means



of our impedance apparatus, because of the crystallization of the electrolytes below 0°C , which is consistent with the DSC results. According to the DSC results, as $\text{Ac}\beta\text{-CD}$ 1.0 and 1.5 are liquid in a wide temperature range, they exhibit a higher ionic conductivity even below 0°C , as shown in **Figure 5**. The ionic conductivities of the $\text{Ac}\beta\text{-CD}$ 1.5, 1.0, 0.5, and 0 composites are 3.2×10^{-4} , 5.1×10^{-4} , 1.6×10^{-3} , and $2.1 \times 10^{-3} \text{ S cm}^{-1}$ at 25°C , respectively. The addition of $\text{Ac}\beta\text{-CD}$ results in the decrease in the conductivity value, ascribable to the formation of an inclusion complex between $\text{Ac}\beta\text{-CD}$ and the TFSA anion. This complex decreases the diffusivity of the component ions, thus decreasing the ionic conductivities. Roy and Roy (2017) used trihexyltetradecylphosphonium chloride as an IL, where a similar decrease in conductivity was observed as the amount of CD increased. The decrease in conductivity will be due to the encapsulation of guest molecules in the hydrophobic cavity of CD (Roy and Roy, 2017).

Figure 8 shows the ionic conductivity at 25°C and viscosity at 30°C as a function of the molar ratio of $\text{Ac}\beta\text{-CD}$. The ionic conductivity monotonously decreases with the $\text{Ac}\beta\text{-CD}$ content as mentioned above. The viscosity values of the $\text{Ac}\beta\text{-CD}$ 1.5, 1.0, 0.5, and 0 composites are 19,000, 1,700, 250, and 60 mPa s at 30°C , respectively. The viscosity values increase steeply as $\text{Ac}\beta\text{-CD}$ is added to the composites. In addition, the conductivities and viscosities are inversely proportional (Salminen et al., 2007). The viscosity increases with CD concentration probably because of the IL and CD interactions and solvation (Roy et al., 2016). Thus, it is considered that the ionic conductivities decrease because of the increase in the viscosities of the composites.



Diffusion Coefficients

The self-diffusion coefficients of $C_3\text{mpyr}^+$ (D_H), Li^+ (D_{Li}), and TFSA^- (D_{TFSA}) for the $[C_3\text{mpyr}][\text{TFSA}]/\text{LiTFSA}$ and $[C_3\text{mpyr}][\text{TFSA}]/\text{LiTFSA}/\text{Ac}\beta\text{-CD}$ composites were determined by means of PFG-NMR at 80°C , as shown in **Figure 9**. The D_H and D_{TFSA} values of these composites are almost the same at 80°C , while the D_{Li} value is lower than those of the D_H and D_{TFSA} values. The increase in the $\text{Ac}\beta\text{-CD}$ content induces a large difference between the D_{Li} value and other values. The apparent lithium transfer number (t_{Li^+}) was calculated from the diffusion coefficient values using Equation (2):

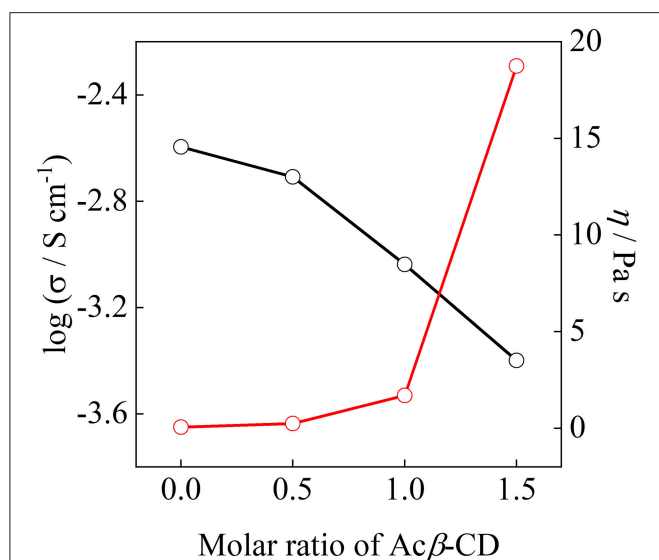


FIGURE 8 | Correlation between ionic conductivity and viscosity for $[C_3mpyr][TFSA]/LiTFSA$ composites and their $Ac\beta$ -CD composites.

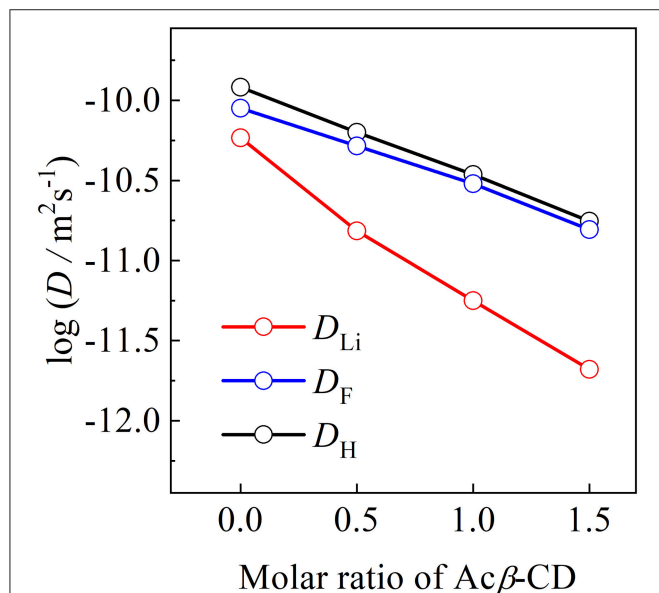


FIGURE 9 | Diffusion coefficients of $[C_3mpyr][TFSA]/LiTFSA$ composites and their $Ac\beta$ -CD composites as a function of mole ratio of $Ac\beta$ -CD.

$$t_{Li^+} = \frac{D_{Li}}{D_{Li} + D_{TFSA} + D_H} \quad (2)$$

Unlike electrochemical techniques, the diffusion coefficients obtained using the PFG-NMR method are derived not only from ionic species but also from non-ionic species (Horiuchi et al., 2017). The t_{Li^+} values of the $Ac\beta$ -CD 1.5, 1.0, 0.5, and 0 composites were 0.06, 0.08, 0.12, and 0.22, respectively. The decrease in the t_{Li^+} values with the increase in $Ac\beta$ -CD content suggests that an inclusion complex will be formed between LiTFSA and $Ac\beta$ -CD. In addition, $Ac\beta$ -CD would form an

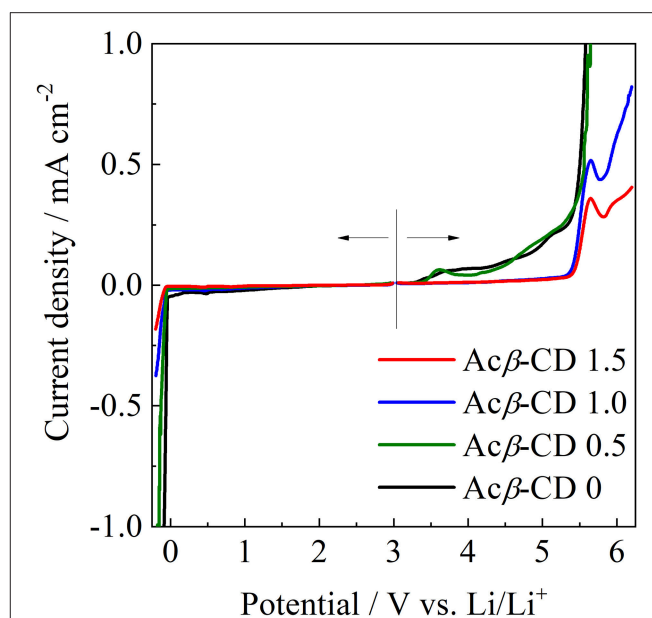


FIGURE 10 | Linear sweep voltammograms of $[C_3mpyr][TFSA]/LiTFSA$ composites and their $Ac\beta$ -CD composites.

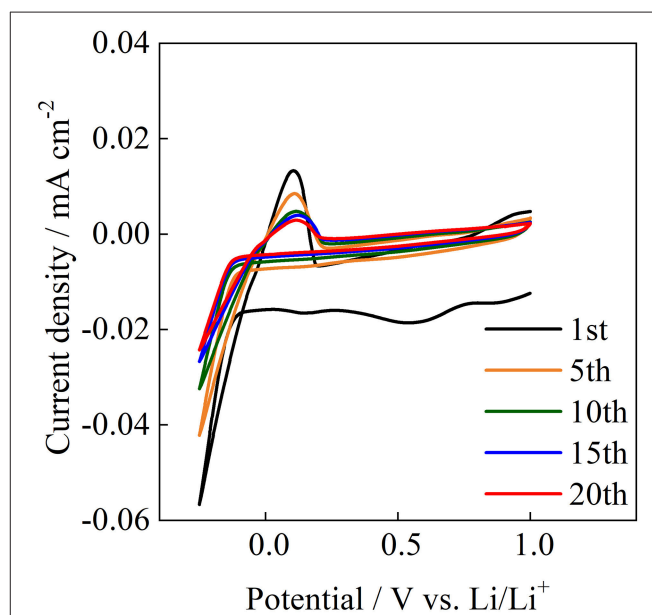


FIGURE 11 | Cyclic voltammograms of $Ac\beta$ -CD 1.0 at 25°C.

inclusion complex with not only LiTFSA but also the aggregation including a Li cation, similar to the combination of two TFSA anions and one Li cation because the large surface charge density of a Li cation induces the formation of cluster ions (Appetecchi et al., 2016).

Electrochemical Properties

The electrochemical stabilities of the $[C_3mpyr][TFSA]/LiTFSA$ and $[C_3mpyr][TFSA]/LiTFSA/Ac\beta$ -CD composites were investigated by LSV on a Ni electrode (from 3 to -0.2 V)

and Pt electrode (from 3 to 6 V) at 60°C. The LSV results are presented in **Figure 10**. The electrochemical window ($EW = E_{\text{anodic}} - E_{\text{cathodic}}$) of all the IL electrolytes was determined from the values for the cathodic (E_{cathodic}) limit at -0.1 mA cm^{-2} and anodic (E_{anodic}) limit at 0.1 mA cm^{-2} . The EW value of $\text{Ac}\beta\text{-CD}$ 0 is 4.6 V vs. Li/Li^+ and that of $\text{Ac}\beta\text{-CD}$ 0.5 is 4.6 V vs. Li/Li^+ , which is almost the same as that of $\text{Ac}\beta\text{-CD}$ 0. The EW values are about 5.5 V vs. Li/Li^+ for both $\text{Ac}\beta\text{-CD}$ 1.0 and 1.5 composites. As the addition amount of $\text{Ac}\beta\text{-CD}$ increases, the oxidation stability improves. This improvement should be based on the formation of an inclusion complex between $\text{Ac}\beta\text{-CD}$ and the TFSA anion because the anodic stability significantly improves, and the cathodic stability is almost the same regardless of the addition of $\text{Ac}\beta\text{-CD}$.

The reversible oxidation and reduction reactions of lithium were examined at room temperature for $\text{Ac}\beta\text{-CD}$ 1.0. **Figure 11** shows the cyclic voltammogram for $\text{Ac}\beta\text{-CD}$ 1.0 on a Ni electrode. $\text{Ac}\beta\text{-CD}$ 1.0 exhibits reduction and oxidation peaks for Li at about -0.1 and 0.1 V vs. Li/Li^+ , respectively. The current density decreases with the cycling number from 1st to 10th. After that, the current density maintains a constant value, and stable reversible redox reactions are observed during 20 cycles. At the initial anodic sweep, an anodic current is observed. This behavior is also observed for pyrrolidinium-based ILs (Towada et al., 2015; Horiuchi et al., 2016). In addition, the maximum current density of the anodic peak slightly shifts to a higher potential value with the increase in cycle number. These results suggest that a solid electrolyte interphase film is formed on the Ni electrode surface (Grande et al., 2015), even in the presence of $\text{Ac}\beta\text{-CD}$.

CONCLUSIONS

The effect of $\text{Ac}\beta\text{-CD}$ on the properties of $[\text{C}_3\text{mpyr}][\text{TFSA}]/\text{LiTFSA}$ was investigated by means of several techniques. The chemical shift of the CF_3 group of the

TFSA anion shifted to a lower magnetic field with the increase in the $\text{Ac}\beta\text{-CD}$ content. With the addition of $\text{Ac}\beta\text{-CD}$ to the IL electrolyte, the T_m of the IL disappeared and the viscosity increased. These results suggest that an inclusion complex is formed between $\text{Ac}\beta\text{-CD}$ and the TFSA anion. In contrast, the t_{Li^+} and D_{Li} values decreased with the increase in the $\text{Ac}\beta\text{-CD}$ content in the composites. The anodic stability of $[\text{C}_3\text{mpyr}][\text{TFSA}]/\text{LiTFSA}$ was significantly improved after adding a certain amount of $\text{Ac}\beta\text{-CD}$. Li plating and stripping in the $[\text{C}_3\text{mpyr}][\text{TFSA}]/\text{LiTFSA}/\text{Ac}\beta\text{-CD}$ composite were repeatedly observed. According to these results, $\text{Ac}\beta\text{-CD}$ will be an interesting additive for improving the electrochemical stability of ILs. It is known that there are three kinds of CD, $\alpha\text{-CD}$, $\beta\text{-CD}$, and $\gamma\text{-CD}$, which have different cavity sizes. The physicochemical properties of various ILs with different anions could be controlled by choosing suitable CD derivatives.

AUTHOR CONTRIBUTIONS

MS and MY-F designed the research. MS prepared the samples and measured the properties. MS and NK carried out the NMR measurements and the data collection. YT, MR, and MY-F participated in the data analysis. MS and MY-F wrote the manuscript.

FUNDING

This work was supported by a Sophia University Special Grant for Academic Research.

ACKNOWLEDGMENTS

We thank Sophia University for instrumental analyses (FAB-MS and elemental analysis).

REFERENCES

- Amajjahe, S., Choi, S., Munteanu, M., and Ritter, H. (2008). Pseudopolyanions based on poly(NIPAAm-co-beta-cyclodextrin methacrylate) and ionic liquids. *Angew. Chem. Int. Ed. Engl.* 47, 3435–3437. doi: 10.1002/anie.200704995
- Amajjahe, S., and Ritter, H. (2008). Anion complexation of vinylimidazolium salts and its influence on polymerization. *Macromolecules* 41, 716–718. doi: 10.1021/ma702271p
- Appetecchi, G. B., D'Annibale, A., Santilli, C., Genova, E., Lombardo, L., Navarra, M. A., et al. (2016). Novel functionalized ionic liquid with a sulfur atom in the aliphatic side chain of the pyrrolidinium cation. *Electrochem. Commun.* 63, 26–29. doi: 10.1016/j.elecom.2015.12.009
- Armand, M., Endres, F., MacFarlane, D. R., Ohno, H., and Scrosati, B. (2009). Ionic-liquid materials for the electrochemical challenges of the future. *Nat. Mater.* 8, 621–629. doi: 10.1038/nmat2448
- Baâzaoui, M., Béjaoui, I., Kalfat, R., Amdouni, N., Hbaieb, S., and Chevalier, Y. (2016). Interfacial properties and thermodynamic behavior of cationic amphiphilic β -cyclodextrins substituted with one or seven alkyl chains. *RSC Adv.* 6, 72044–72054. doi: 10.1039/C6RA10597A
- Chen, R., Lai, J., Li, Y., Cao, M., Chen, S., and Wu, F. (2016). β -Cyclodextrin coated lithium vanadium phosphate as novel cathode material for lithium ion batteries. *RSC Adv.* 6, 103364–103371. doi: 10.1039/C6RA22400H
- Crini, G. (2014). Review: a history of cyclodextrins. *Chem. Rev.* 114, 10940–10975. doi: 10.1021/cr500081p
- Franco, A. A. (2015). *Rechargeable Lithium Batteries*. Cambridge: Woodhead/Elsevier Science.
- Grande, L., von Zamory, J., Koch, S. L., Kalhoff, J., Paillard, E., and Passerini, S. (2015). Homogeneous lithium electrodeposition with pyrrolidinium-based ionic liquid electrolytes. *ACS Appl. Mater. Interfaces* 7, 5950–5958. doi: 10.1021/acsami.5b00209
- He, Y., Chen, Q., Xu, C., Zhang, J., and Shen, X. (2009). Interaction between ionic liquids and β -cyclodextrin: a discussion of association pattern. *J. Phys. Chem. B* 113, 231–238. doi: 10.1021/jp808540m
- Horiuchi, S., Yoshizawa-Fujita, M., Takeoka, Y., and Rikukawa, M. (2016). Physicochemical and electrochemical properties of *N*-methyl-*N*-methoxymethylpyrrolidinium bis(fluorosulfonyl)amide and its lithium salt composites. *J. Power Sources* 325, 637–640. doi: 10.1016/j.jpowsour.2016.06.087
- Horiuchi, S., Zhu, H., Forsyth, M., Takeoka, Y., Rikukawa, M., and Yoshizawa-Fujita, M. (2017). Synthesis and evaluation of a novel pyrrolidinium-based zwitterionic additive with an ether side chain for ionic liquid electrolytes in high-voltage lithium-ion batteries. *Electrochim. Acta* 241, 272–280. doi: 10.1016/j.electacta.2017.04.165

- Ishikawa, M., Sugimoto, T., Kikuta, M., Ishiko, E., and Kono, M. (2006). Pure ionic liquid electrolytes compatible with a graphitized carbon negative electrode in rechargeable lithium-ion batteries. *J. Power Sources* 162, 658–662. doi: 10.1016/j.jpowsour.2006.02.077
- Laus, G., Bentivoglio, G., Kahlenberg, V., Griesser, U. J., Schottenberger, H., and Nauer, G. (2008). Syntheses, crystal structures, and polymorphism of quaternary pyrrolidinium chlorides. *CrystEngComm* 10, 748–752. doi: 10.1039/b718917f
- Li, X., Zhang, Z., Li, S., Yang, K., and Yang, L. (2017). Polymeric ionic liquid-ionic plastic crystal all-solid-state electrolytes for wide operating temperature range lithium metal batteries. *J. Mater. Chem. A* 5, 21362–21369. doi: 10.1039/C7TA04204C
- Liu, Z.-T., Shen, L.-H., Liu, Z.-W., and Lu, J. (2009). Acetylation of β -cyclodextrin in ionic liquid green solvent. *J. Mater. Sci.* 44, 1813–1820. doi: 10.1007/s10853-008-3238-1
- Matsumoto, H., Sakaebae, H., Tatsumi, K., Kikuta, M., Ishiko, E., and Kono, M. (2006). Safety assessment of ionic liquid-based lithium-ion battery prototypes. *J. Power Sources* 160, 1308–1313. doi: 10.1016/j.jpowsour.2006.02.018
- Narita, A., Shibayama, W., Sakamoto, K., Mizumo, T., Matsumi, N., and Ohno, H. (2006). Lithium ion conduction in an organoborate zwitterion–LiTFSI mixture. *Chem. Commun.* 1926–1928. doi: 10.1039/B517019B
- Nishimura, N., and Ohno, H. (2014). 15th anniversary of polymerised ionic liquids. *Polymer* 55, 3289–3297. doi: 10.1016/j.polymer.2014.02.042
- Ohno, H. (2011). *Electrochemical Aspects of Ionic Liquids, Second Ed.* Hoboken, NJ: John Wiley & Sons, Inc.
- Ohno, H., and Fukaya, Y. (2009). Task specific ionic liquids for cellulose technology. *Chem. Lett.* 38, 2–7. doi: 10.1246/cl.2009.2
- Qian, W., Texter, J., and Yan, F. (2017). Frontiers in poly(ionic liquid)s: syntheses and applications. *Chem. Soc. Rev.* 46, 1124–1159. doi: 10.1039/C6CS00620E
- Roy, A., and Roy, M. N. (2017). Cage to cage study of ionic liquid and cyclic oligosaccharides to form inclusion complexes. *RSC Adv.* 7, 40803–40812. doi: 10.1039/C7RA08397A
- Roy, A., Saha, S., Datta, B., and Roy, M. N. (2016). Insertion behavior of imidazolium and pyrrolidinium based ionic liquids into α and β -cyclodextrins: mechanism and factors leading to host–guest inclusion complexes. *RSC Adv.* 6, 100016–100027. doi: 10.1039/C6RA19684E
- Salminen, J., Papaiconomou, N., Kumar, R. A., Lee, J.-M., Kerr, J., Newman, J., et al. (2007). Physicochemical properties and toxicities of hydrophobic piperidinium and pyrrolidinium ionic liquids. *Fluid Phase Equilibria* 261, 421–426. doi: 10.1016/j.fluid.2007.06.031
- Seki, S., Kobayashi, Y., Miyashiro, H., Ohno, Y., and Mita, Y., Terada, N., et al. (2008). Compatibility of *N*-methyl-*N*-propylpyrrolidinium cation room-temperature ionic liquid electrolytes and graphite electrodes. *J. Phys. Chem. C* 112, 16708–16713. doi: 10.1021/jp805403e
- Seki, S., Ohno, Y., Miyashiro, H., Kobayashi, Y., Usami, A., Mita, Y., et al. (2008). Quaternary ammonium room-temperature ionic liquid/lithium salt binary electrolytes: electrochemical study. *J. Electrochem. Soc.* 155, A421–A427. doi: 10.1149/1.2899014
- Silva, O. F., Fernández, M. A., Pennie, S. L., Gil, R. R., and de Rossi, R. H. (2008). Synthesis and characterization of an amphiphilic cyclodextrin, a micelle with two recognition sites. *Langmuir* 24, 3718–3726. doi: 10.1021/la702962f
- Szejtli, J. (1998). Introduction and general overview of cyclodextrin chemistry. *Chem. Rev.* 98, 1743–1754. doi: 10.1021/cr970022c
- Tanner, J. E., and Stejskal, E. O. (1968). Restricted self-diffusion of protons in colloidal systems by the pulsed-gradient, spin-echo method. *J. Chem. Phys.* 49, 1768. doi: 10.1063/1.1670306
- Towada, J., Karouji, T., Sato, H., Kadoma, Y., Shimada, K., and Ui, K. (2015). Charge–discharge characteristics of natural graphite electrode in *N,N*-diethyl-*N*-methyl-*N*-(2-methoxyethyl)ammonium bis(trifluoromethylsulfonyl)amide containing lithium ion for lithium-ion secondary batteries. *J. Power Sources* 275, 50–54. doi: 10.1016/j.jpowsour.2014.10.101
- Wu, A., Lu, F., Sun, P., Qiao, X., Gao, X., and Zheng, L. I. (2017). Low-molecular-weight supramolecular ionogel based on host–guest interaction. *Langmuir* 33, 13982–13989. doi: 10.1021/acs.langmuir.7b03504
- Wu, T.-Y., Su, S.-G., Wang, H.-P., Lin, Y.-C., Gung, S.-T., Lin, M.-W., et al. (2011). Electrochemical studies and self diffusion coefficients in cyclic ammonium based ionic liquids with allyl substituents. *Electrochim. Acta* 56, 3209–3218. doi: 10.1016/j.electacta.2011.01.040
- Yabuuchi, N., and Ohzuku, T. (2003). Novel lithium insertion material of $\text{LiCo}_{1/3}\text{Ni}_{1/3}\text{Mn}_{1/3}\text{O}_2$ for advanced lithium-ion batteries. *J. Power Sources* 119–121, 171–174. doi: 10.1016/S0378-7753(03)00173-3
- Yang, B., Li, C., Zhou, J., Liu, J., and Zhang, Q. (2014). Pyrrolidinium-based ionic liquid electrolyte with organic additive and LiTFSI for high-safety lithium-ion batteries. *Electrochim. Acta* 148, 39–45. doi: 10.1016/j.electacta.2014.10.001
- Yoon, H., Best, A. S., Forsyth, M., MacFarlane, D. R., and Howlett, P. C. (2015). Physical properties of high Li-ion content *N*-propyl-*N*-methylpyrrolidinium bis(fluorosulfonyl)imide based ionic liquid electrolytes. *Phys. Chem. Chem. Phys.* 17, 4656–4663. doi: 10.1039/C4CP05333H
- Yoshizawa, M., Narita, A., and Ohno, H. (2004). Design of ionic liquids for electrochemical applications. *Aust. J. Chem.* 57, 139–144. doi: 10.1071/CH03240
- Yoshizawa-Fujita, M., Tamura, T., Takeoka, Y., and Rikukawa, M. (2011). Low-melting zwitterion: effect of oxyethylene units on thermal properties and conductivity. *Chem. Commun.* 47, 2345–2347. doi: 10.1039/C0CC03754K
- Yuan, J., Mecerreyes, D., and Antonietti, M. (2013). Poly(ionic liquid)s: an update. *Prog. Polym. Sci.* 38, 1009–1036. doi: 10.1016/j.progpolymsci.2013.04.002
- Zhang, W., Yuan, C., Guo, J., Qiu, L., and Yan, F. (2014). Supramolecular ionic liquid gels for quasi-solid-state dye-sensitized solar cells. *ACS Appl. Mater. Interfaces* 6, 8723–8728. doi: 10.1021/am501523x
- Zhu, Z., Qilu, Z. D., and Yu, H., (2014). Preparation of spherical hierarchical $\text{LiNi}_{0.5}\text{Mn}_{1.5}\text{O}_4$ with high electrochemical performances by a novel composite co-precipitation method for 5 V lithium ion secondary batteries. *Electrochim. Acta* 115, 290–296. doi: 10.1016/j.electacta.2013.10.167

Conflict of Interest Statement: The authors declare that the research was conducted in the absence of any commercial or financial relationships that could be construed as a potential conflict of interest.

Copyright © 2019 Suzuki, Kurahashi, Takeoka, Rikukawa and Yoshizawa-Fujita. This is an open-access article distributed under the terms of the Creative Commons Attribution License (CC BY). The use, distribution or reproduction in other forums is permitted, provided the original author(s) and the copyright owner(s) are credited and that the original publication in this journal is cited, in accordance with accepted academic practice. No use, distribution or reproduction is permitted which does not comply with these terms.